Application of the Factorial Design Technique for the Optimization of the Chemical Isolation Process of Lead in Environmental Analyzes

Gonçalves, MCP[1], Rodrigues, FW[2], Romanelli, JP[3]

[1]Science and Technology Institute, Federal University of Alfenas, José Aurélio Vilela Road 11999, Km 533, CEP 37715-400, Poços de Caldas, MG, Brazil.
[2,3]Federal University of São Carlos, 13565-905, São Carlos-SP, Brazil.

Abstract*—Nuclear energy plays a key role in long-term development plans and can guarantee the supply of electricity to some regions. On the other hand, the implementation of these projects tends to require long maturation periods, require high investment costs and may be a source of pollutants, such as Lead (Pb). For this reason, the periodic environmental monitoring of the concentration of pollutants becomes necessary, according to the current legislation. Thus, the present work presents as a proposal a method of optimization of Pb quantification in environmental analyzes. The study was developed through the monitoring of wastewater samples from INB – Indústrias Nucleares do Brasil. From the Fractional Factorial Design(FFD) the most representative variables of the Pb isolation process were determined, and through the Central Composite Design (CCD) the response surface was found, generating a regression model that represents the system. The results indicated that the optimization of the chemical yield of Pb is associated to the higher dosages of Nitrilotriacetic Acid (NTA) and Sulfuric Acid (H_2SO_4) in the samples. The optimum yield condition was obtained in the region of 200 ml of H_2SO_4 and 4.0 g of NTA, considering the range tested. The proposal proved to be effective for the validation tests of the model, obtaining an increase of up to 32% in the Pb yields of the analyzes.*

Keywords*—*Chemical Yield, Environmental Analyzes, Lead, Nuclear Power, Response Surface.

I. INTRODUCTION

The generation of electricity from nuclear sources can be considered advantageous and represent a viable strategy of diversification of the energy matrix in some countries [1,2], meeting the goals of reducing greenhouse gas emissions compatible with the Kyoto Protocol [3,4]. Nuclear energy plays a key role in long-term development plans and can guarantee energy supply for some regions [5]. On the other hand, the implementation of these projects tends to require long maturation periods, from the installation of the plant until its operation, in addition to requiring high investment costs and representing sources of environmental degradation [4,6,7].

Currently in Brazil nuclear sources have little expressiveness in the electric matrix, but this scenario tends to undergo changes until the year 2050 [8]. The Brazilian government plans to build new nuclear plants by 2030 [6,9], which should represent an increase of approximately 6 GW in capacity country [6,10].

The process of generating energy from nuclear sources occurs through nuclear fission in reactors, which are fed by fuels from the extraction of uranium ore [11,12,13,14,15]. From the mining stage to the production of nuclear fuel, innumerable pollutants from soil, air and water, especially heavy metals, such as lead, which has high toxicity and may cause serious social and environmental impacts [16,17,18,19,20,21,22].

In the case of wastewater from nuclear activities, there is a demand for specific treatments so that they can meet the quality adjustments [23,24], as established by Resolution No. 430 of the Conselho Nacional de Meio Ambiente – CONAMA [25]. According to this resolution, release of effluents containing Pb to water bodies or collection systems must comply with the maximum acceptable limit of 0,5 $mg.L^{-1}$ [25]. Therefore, periodic environmental analyzes must be carried out to monitor and control the concentration of Pb according to current legislation [26,27,28,29]. Such analyzes involve a methodology of isolation and quantification, having as principle the separation of the lead from the other elements, besides the separation between them by selective precipitation aiming the determination of the yield of Pb in the samples.

Thus, the present study proposes the optimization of the lead insulation process in environmental analyzes, as a way to improve the efficiency of the quantification of Pb yields, in order to guarantee reliable results that comply with the norms of the current legislation. The Fractional Factorial Design (FFD) was used to determine the most representative variables of the process [30,31,32,33,34], in order to verify the relevant sources of interference of the method employed. The Central

Composite Design (CCD) was used to find the response surface where the yield of Pb is maximum, generating a regression model that represents the system [35,36,37,38,39,40].

II. MATERIAL AND METHODS

The execution of the factorial design was started with the collection of a sample composed of water (60 liters), collected from several monitoring points of the company Indústrias Nucleares do Brasil (INB), a unit of Caldas-MG. The sample was filtered and reduced in hotplate up to 30 liters. In the first step of the optimization, four variables were selected to be tested in the chemical insulation of lead (Pb): i) addition order of Nitrilotriacetic Acid (NTA), Sodium Hydroxide (NaOH) 6 $mol.L^{-1}$, Ammonium Sulfate (NH_4SO_4) 25 $mg.L^{-1}$ and heated distilled water; ii) NTA dosage; iii) dosage of Sulfuric Acid (H_2SO_4) 3 $mol.L^{-1}$, and iv) dosage of Sodium Sulphide (Na_2S) 1 $mol.L^{-1}$.

According to the Fractional Factorial Design procedures, the number of experiments to be performed is of the order of 2^{n-1}, where n represents the number of variables listed [30]. Thus, in this study, 8 experiments (2^{4-1}) were performed in triplicate, totaling 24 tests. The FFD codifies the possibilities to be tested in the level tests. In this case, the level -1 represents the currently applied conditions and the level +1 the new conditions tested. Table 1 shows the cataloged variables and their respective levels.

TABLE 1
VARIABLES LISTED AND THEIR RESPECTIVE LEVELS.

Variable	Level
A) Order of addition of the reagents: nitrilotriacetic acid (NTA), sodium hydroxide (NaOH) 6 $mol.L^{-1}$, ammonium sulfate (NH_4SO_4) 25 $mg.L^{-1}$ and heated distilled water	**Level (-1):** 1º NTA, 2º NaOH, 3º NH_4SO_4, 4º heated distilled water (current order). **Level (+1):** 1º heated distilled water, 2º NaOH, 3º NTA, 4º NH_4SO_4 (new order).
B) Dosing of NTA	**Level (-1):** 2,0 g of NTA (current dosage). **Level (+1):** 4,0 g of NTA (new dosage).
C) Dosing of H_2SO_4 3 $mol.L^{-1}$	**Level (-1):** 50 ml of H_2SO_4 0,1 $mol.L^{-1}$ (current volume). **Level (+1):** 150 ml of H_2SO_4 0,1 $mol.L^{-1}$ (new volume).
D) Dosing of Na_2S 1 $mol.L^{-1}$	**Level (-1):** 1,0 ml of Na_2S (current volume). **Level (+1):** 3,0 ml of Na_2S (new volume).

The next step consisted in inserting all variables and their respective levels into Minitab software (version 16.2.4.4), in order to obtain an array with all possible combinations of experimental tests (Table 2) [41].

TABLE 2
EXPERIMENTAL MATRIX OF THE FRACTIONAL FACTORIAL DESIGN FOR Pb.

Experiment	Level	NTA (g)	H_2SO_4 (ml)	Na_2S(ml)
1	+1	2	50	3
2	-1	2	50	1
3	-1	4	150	1
4	+1	4	150	3
5	+1	4	50	1
6	-1	2	150	3
7	+1	2	150	1
8	-1	4	50	3

From the matrix obtained, the tests of isolation and quantification of Pb with the 24 samples were performed, following the analysis procedures described below:

1. After the filtration initially described, the sample was transferred to 24 beakers of 2 liters, each containing 1 liter of sample;
2. Then 1 mL of 20 $mg.mL^{-1}$ Barium solution and 1 mL of 20 $mg.mL^{-1}$ Lead solution were added with a micropipettor;
3. With dispensing, 5 mL of Citric Acid solution ($C_6H_8O_7$) 1 $mol.L^{-1}$ and 2 drops of 0.1% Methyl Red in each beaker were added. The pH of the sample was adjusted between 6.0 and 7.0 with Ammonium Hydroxide (NH_4OH) and Nitric Acid (HNO_3) 5 $mol.L^{-1}$ slowly, until turning from red to yellow, using calibrated Phmetro;
4. To each beaker were added 50 ml of Sulfuric Acid solution (H_2SO_4) 3 $mol.L^{-1}$, with stirring, and the solution was heated to boiling and allowed to settle until the following day;
5. The supernatant was then drained by siphoning and the precipitate transferred quantitatively into the glass centrifuge tube using osmosis purified water;
6. The sample was centrifuged for 10 minutes at 2000 RPM and the supernatant discarded by siphoning. This was done with 20 ml of H_2SO_4 solution 0.1 $mol.L^{-1}$ added to the precipitate, while the supernatant was centrifuged and discarded by siphoning again;
7. To the precipitated was added 2.0 g of Nitrilotriacetic Acid (NTA), 10 mL of Sodium Hydroxide solution (NaOH) 6 $mol.L^{-1}$, 50 mL of distilled water and 5 mL of Ammonium Sulfate $(NH_4)_2SO_4$) 25 $mg.mL^{-1}$;
8. The tubing solution was heated in a water bath at approximately 90 °C for 15 minutes until the precipitate dissolved completely. Then, the pH of the sample was adjusted by adding glacial Acetic Acid to pH between 4.0 and 4.5 and the solution was held until the following day;
9. The solution obtained was centrifuged, the supernatant was transferred to a 250 mL beaker to separate it from the precipitate and it was reserved in tubes;
10. In each of the supernatants obtained was added 1 mL of Sodium Sulfate (Na_2S) solution 1 $mol.L^{-1}$. These were then left in a water bath at 90 °C for approximately 15 minutes;
11. After cooling the samples in the chambers, the solutions obtained were centrifuged, the supernatant was discarded by siphoning and the precipitate was washed with 50 ml of distilled water. The sample was then centrifuged again and the supernatant discarded by siphoning. To the precipitate was added 10 mL of HNO_3 solution 5 $mol.L^{-1}$;
12. The solution was taken in a water bath at approximately 90 °C and waited from 100 to 120 minutes until the total Lead Sulphide formation reaction occurred, which is indicated by the absence of dark, sulfur-forming spots. Each of the samples was screened on white strip paper and the filter was washed 3 times with heated distilled water. They were then left in a water bath for 10 minutes;
13. The pH of the resulting solution was adjusted between 4.0 and 4.5 with Ammonium Acetate solution (NH_4CH_3COO) 40%. To each sample was added 1 mL of Bismuth solution 5 $mg.mL^{-1}$ and 2 mL of Sodium Chromate solution (Na_2CrO_4) 30%;
14. The material was filtered using a vacuum filtration kit, with 0.45 μm membrane filter and diameter Ø = 47 mm, previously weighed in analytical balance. The precipitate was washed with distilled water, the filter was removed from the Kit and stoved at 60 °C for 90 minutes;
15. Finally, the filter was removed from the oven and placed in desiccator for 10 minutes. The samples were taken from the desiccator, weighed and the yield was calculated considering the added standard mass equal to 31 mg. The gravimetric yield was calculated from the Equation:

$$Y_{grav}\ (\%) = 100\frac{M_p - M_f}{M_a} \quad (1)$$

Where: M_p is the mass of the filter with precipitate;

M_f is the mass of the filter;

M_a is the theoretical mass of Lead standard (31 mg).

16. After the previous tests were carried out to determine the response surface of the CCD, the filters were digested in a microwave oven and then analyzed in an Inductively Coupled Plasma Atomic Emission Spectrometer (ICP). The chemical yield was calculated from the Equation:

$$Y_{chem}\ (\%) = \frac{C_{Pb}\ .V_f}{\frac{MM_{Pb}\ .\ m_{PbCrO\ 4}}{MM_{PbCrO\ 4}}}\ .100 \quad (2)$$

Where: C_{Pb} is the concentration of Pb ($g.L^{-1}$);
V_f is the volumetric flask volume (0.05 L);
MM_{Pb} is the molar mass of Pb (207.19 $g.mol^{-1}$);
m_{PbCrO_4} is the mass of Lead Chromate (0.031 g);
MM_{PbCrO_4} is the molar mass of Lead Chromate (323.2 $g.mol^{-1}$).

2.1 Validation of the model

To validate the model found by the response surface of the Central Composite Design (CCD), new tests were performed for four different samples of wastewater under the current conditions (50 mL of H_2SO_4 and 2 g of NTA) and under the optimum conditions established by the model. The assays followed the same procedure described previously for the chemical isolation of Pb by selective precipitation.

III. RESULTS AND DISCUSSION

After the Pb isolation for the 24 samples of FFD, the average gravimetric yields were obtained in each of the experimental conditions (Equation 1). In the next step, the variables were coded at levels -1 and +1, as described in Table 1, obtaining a new coefficient matrix. From the possible combinations between the four variables selected in the coded levels, the contrasts involved in the design and their respective percentages of contribution were calculated (Table 3).

TABLE 3
CONTRASTS CALCULATED FOR THE DEVELOPMENT OF THE FRACTIONAL FACTORIAL DESIGN FOR Pb.

Combinations	A+BCD	B+ACD	C+ABD	D+ABC	AB+CD	AC+BD	AD+BC
Contrasts	-5,88	-3,88	1,04	-2,29	1,79	0,04	-1,29
Contrasts (%)	56,82	24,72	1,78	8,64	5,28	0,003	2,746

To verify which of the selected variables have a significant effect on the system, the confidence interval of the contrast error was calculated. First, the number of degrees of freedom (DF) and the quadratic sum of the pure error (QSPE) were calculated. From the DF and QSPE values we found the experimental variance (S^2), the experimental error (S), the contrast error (S_c) and finally the confidence interval of the contrast error (I_{S_c}) for a 95% confidence interval, as shown in Equations (3), (4), (5) and (6), respectively. All statistical data obtained are presented in Table 4.

$$S^2 = \frac{\sum GL \cdot SQEP}{\sum GL} \quad (3)$$

$$S = \sqrt{S^2} \quad (4)$$

$$S_c = \frac{\sqrt{S^2}}{3} \quad (5)$$

$$I_{S_c} = t \cdot S_c \quad (6)$$

TABLE 4
STATISTICAL DATA FOUND FOR Pb ANALYSIS

Experimental Variance (S^2)	10,20
Experimental Error (S)	3,20
Contrast Error (S_c)	1,80
Confidence Interval of the Contrast Error (I_{S_c})	3,30

As the confidence interval for the Contrast Error found was 3.30, only the contrasts larger than this value in modulus will be significant. Thus, as shown in Table 4, only the interactions A+BCD (contrast: -5.88) and B+ACD (contrast: -3.88) are relevant.

As the probability of occurrence of a third-order interaction is minimal, it is considered that only A and B are influencing the analysis, only the dosage of H_2SO_4 (56.8%) and NTA (24.7%). According to researches by Ozer and Guçer (2011) [42], the volume of Sulfuric Acid presented as a relevant variable in the digestion process of Pb samples, since it can participate in the formation of Lead Sulphate precipitate. Studies by Sakurai et al. (2006) [43] also reported the significant effect of H_2SO_4 on the plastic digestion for the determination of Pb in a microwave oven. No results were found for NTA in the literature.

To visualize what was found by the previous calculations, a graph of cubes was constructed (Fig. 1), with the aid of the software OriginPro 9.1.0, which presents the variables under study and their respective levels coded as a function of the obtained Pb yield [44].

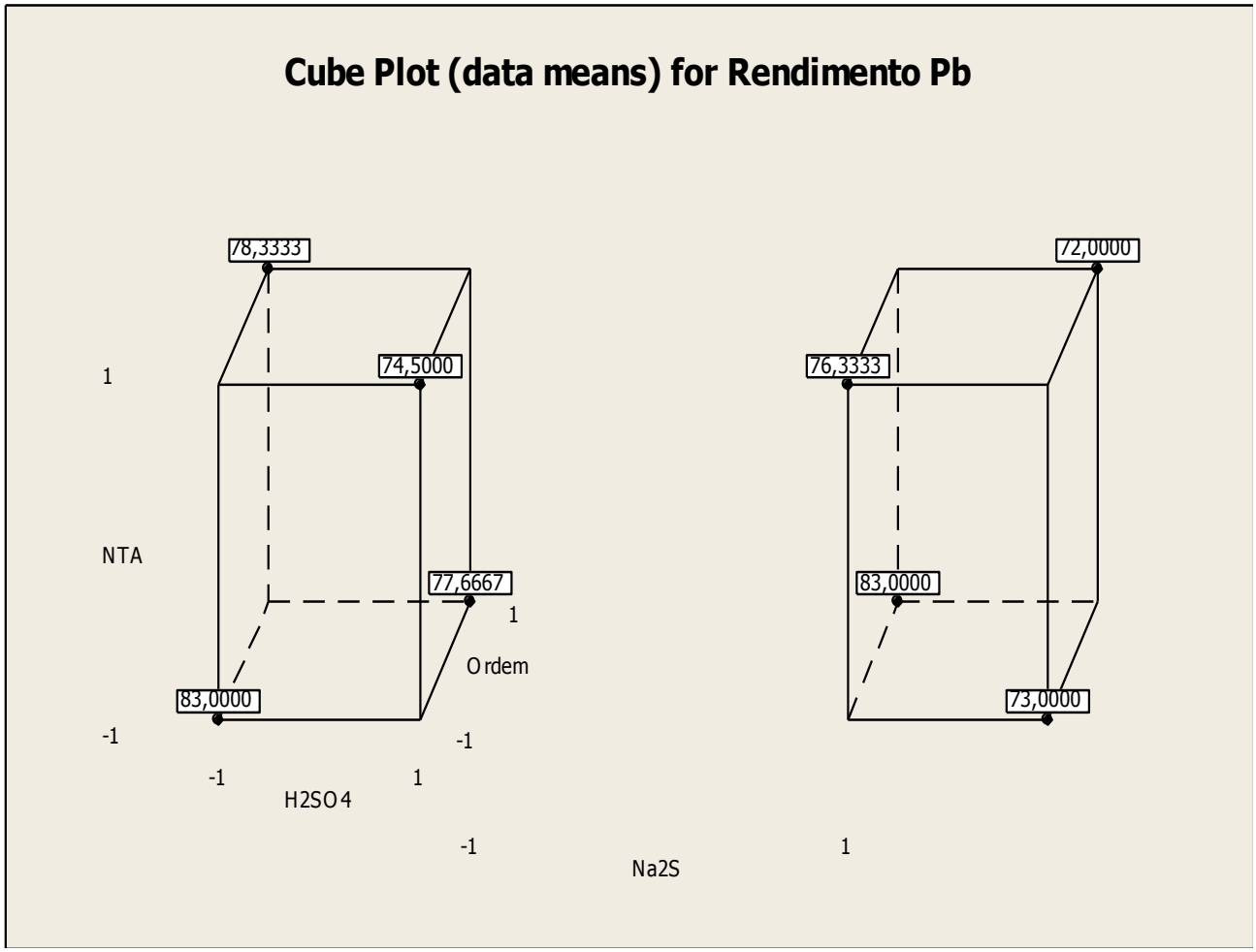

FIGURE 1. CUBE PLOT FOR Pb YIELD.

Fig. 1 shows that level -1 (current dosage) for H_2SO_4 has a higher average yield than level +1 (new dosage) for the same reagent, thus contributing to the maximization of Pb yield at level -1. For the NTA dosage, the level -1 also has an average yield greater than the level +1, evidencing that the level -1 is more advantageous for the increase of the Pb yield.

3.1 Response surface

The initial proposal to define the response surface of the FFD in question was to employ a Central Composite Design (CCD) with two variables (dosage of Sulfuric Acid and NTA). This type of experiment employs compounds with a central point in order to identify the best working conditions of an analytical method. The variables are tested in 5 different levels, ranging from $-\sqrt{2}$ to $\sqrt{2}$ [30].

By the established method, the coded interval (Ic) should be 2.83 for both H_2SO_4 and NTA dosage. The actual interval (Ir) was defined as 200 ml for H_2SO_4 and 3.5 g for NTA. From the values of Ic, Ir and the levels coded according to the Central Composite Design were calculated the actual levels. Table 5 shows the actual and coded levels defined by the CCD technique.

TABLE 5
CODED AND ACTUAL LEVELS ESTABLISHED BY THE CENTRAL COMPOSITE DESIGN METHOD.

Experiment	Coded Levels		Real Levels	
	Sulfuric Acid 3 mol.L^{-1}	NTA	Sulfuric Acid 3 mol.L^{-1} (ml)	NTA (g)
1	-1	-1	29,3	1,0
2	0	0	100,0	2,3
3	0	-1,4142	100,0	0,5
4	-1	1	29,3	3,5
5	-1,4142	0	0,0	2,3
6	1	-1	170,7	1,0
7	0	1,4142	100,0	4,0
8	1	1	170,7	3,5
9	1,4142	0	200,0	2,3

After the experiments were carried out by the method described for the lead insulation, the filters were obtained in a microwave oven and afterwards an Atomic Emission Spectrometer with Inductively Coupled Plasma (ICP). This procedure was performed in order to verify if the filters only have Lead Chromate (resulting from the analysis), or if any interfering substances are still present that were not totally removed in the isolation procedure and are contributing to the different gravimetric yield got from the chemical, obtained by quantification of Pb in the ICP, masking the true result of the analysis.

After the tests, the gravimetric yields were calculated by the Equation (1) and the chemical yields by Equation (2) of the methodology. The results indicated differences ranging from 5.6 to 33.6% among the yields obtained by gravimetry and quantification of Lead. The systematic difference observed, always with the gravimetric yield greater than the chemical, made it possible to list some possibilities on the origin of the difference, such as the addition of Bismuth solution 5 mg.L^{-1} in the Pb insulation and the residual moisture contained in the due to their drying temperature (60 °C), which may be contributing to a larger mass in the filter. Because the results obtained by quantifying Pb in ICP are more accurate than those found only by gravimetry, it was decided to use the results of chemical yield for the realization of the CCD.

With the execution of the method, it was verified that only the variables NTA and the interaction Sulfuric Acid*NTA are significant for the model. In this way, the other variables and interactions were extracted, being possible to obtain in the software Minitab 16.2.4.4 the following response surface model, which results in the conditions that provide the highest yields [41].

$$\text{Pb Yield } (\%) = 63{,}6828 + 3{,}7383.\,X_1 + 3{,}4385.\,(X_1X_2) \quad (7)$$

Where X_1 and X_2 are the coded levels of NTA and Sulfuric Acid, respectively.

Analyzing the model obtained, the greatest influence of the NTA variable (higher coefficient) is verified, although the interaction between the variables was also significant, evidencing that the response presents a distinct tendency, according to the established levels. Both variables show a positive coefficient, indicating that the higher the levels, the higher the yield. It is noteworthy that Sulfuric Acid alone was not significant.

Studies by Ozer and Guçer (2011), Savic et al. (2014) and Zare-Dorabei et al. (2016), involving Pb analyzes, also demonstrated the direct proportionality relation in their response surface models, since the variables were significant and positive coefficients, therefore, the higher their levels, the greater the associated response [42,45,46]. The response surface graph for the maximization of the chemical yield of Pb was elaborated as a function of the NTA and H_2SO_4 dosage, through the OriginPro 9.1.0 software, as shown in Fig. 2 [44].

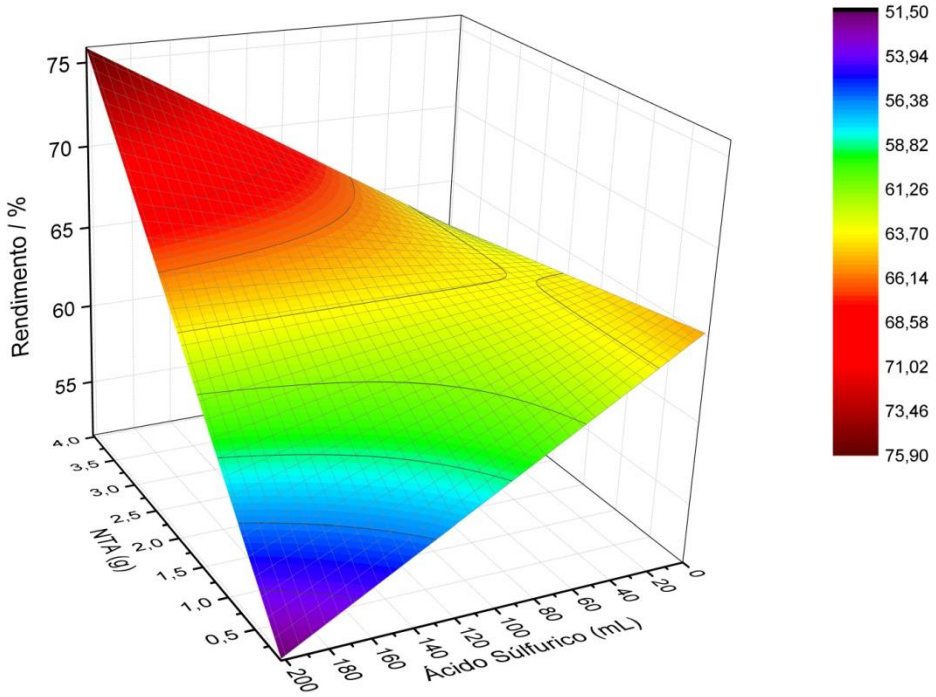

FIGURE 2. RESPONSE SURFACE OBTAINED FOR THE CHEMICAL LEAD YIELD AS A FUNCTION OF THE NTA AND SULFURIC ACID 3 mol.L^{-1} DOSAGES.

Fig. 2 shows that higher concentrations of H_2SO_4 and NTA lead to higher yields, so the optimum condition in which the highest chemical yield of Pb for the range tested would be obtained in the region of 200 ml of H_2SO_4 and 4.0 g of NTA. It is worth mentioning that the current methodology makes the dosage of 2 g of NTA and 50 mL of Sulfuric Acid, which corresponds to a yield of about 62%.

3.2 Validation of the model

The results found for the validation tests of the response surface model for the current dosage (50 ml of H_2SO_4 and 2 g of NTA) and for the new dosage (200 ml of H_2SO_4 and 4 g of NTA) showed that after applying the optimum conditions established by the response surface model obtained there was an increase of up to 32% in the chemical yields of those samples. These results can validate the model found and confirm the significant improvement that the application of the Factorial Design provides to the chemical isolation of Lead and optimizes the yields resulting from the analyzes.

IV. CONCLUSION

- The results of the optimization of the chemical isolation of Pb through the FFD showed that only the H_2SO_4 dosage and the NTA dosage of the isolation methodology influenced the analysis;
- By performing the CCD to obtain the response surface, it was verified that only the variation in the NTA dosage and in the NTA/Sulfuric Acid interaction were significant;
- After the exclusion of the non-significant variables, the response surface showed that the higher the NTA and H_2SO_4 dosage, the higher the associated chemical Pb yield. The optimal condition at which the highest chemical yield of Pb is obtained for the range tested is the region close to 200 ml of H_2SO_4 and 4.0 g of NTA;
- The variable H_2SO_4 dosage alone was not significant in obtaining the response surface, only the NTA/H_2SO_4 association showed influence in the analysis;
- Validation tests of the response surface model showed an increase of up to 32% in the chemical yields of the samples. These results confirm the optimization of the yields that the application of the Factorial Design provided to the chemical isolation of Pb.

ACKNOWLEDGMENTS

The authors thank Indústrias Nucleares do Brasil S.A. for the support offered for the development of the work.

REFERENCES

[1] D.S. Siqueira,"Análise energética e exergética de uma usina nuclear com reator PWR",Msc. Thesis, Federal University of Itajubá, 2016.

[2] K. Vellingiri, K.H. Kim, A. Pournara, A. Deep, "Towards high-efficiency sorptive capture of radionuclides in solution and gas", Progress in Materials Science, vol. 94, pp. 1-67, 2018.

[3] Intergovernmental Panel on Climate Change - IPCC. "Contribution of Working Group III to the Fifth Assessment Report of the Intergovernmental Panel on Climate Change",Available in:
<https://www.ipcc.ch/pdf/assessment-report/ar5/wg3/ipcc_wg3_ar5_full.pdf>. Access in:August 18, 2017.

[4] Y. Fukaya,M. Goto,"Sustainable and safe energy supply with seawater uranium fueled HTGR and its economy". Annals of Nuclear Energy, vol. 99, pp. 19-27, 2017.

[5] K. Saidi, B. Mbarek, "Nuclear energy, renewable energy, CO_2 emissions, and economic growth for nine developed countries: Evidence from panel Granger causality tests", Progress Nuclear Energy vol. 88, pp. 364, 2016.

[6] Empresa de Pesquisa Energética – EPE,"Plano Nacional de Energia 2030: Geração Termonuclear. Ministério de Minas e Energia (MME)",Available in: <http://www.epe.gov.br/PNE/20080512_7.pdf>. Access in: January 11, 2017.

[7] Z.M. Baskurt, C.C. Aydin, "Nuclear power plant site selection by Weighted Linear Combination in GIS environment, Edirne, Turkey", Progress in Nuclear Energy, vol. 104, pp. 85-101, 2018.

[8] A.F.P. Lucena, L. Clarke, R. Schaeffer, A. Szklo, P.R.R. Rochedo, L.P.P. Nogueira, K. Daenzer, A. Gurgel, A. Kitous, T. Kober, "Climate policy scenarios in Brazil: A multi-model comparison for energy", Energy Economics vol. 56, pp. 564, 2016.

[9] R.L.P. Dos Santos, L.P. Rosa, M.C. Arouca, A.E.D. Ribeiro, "The importance of nuclear energy for the expansion of Brazil's electricity grid', ENERGY POLICY, vol. 60, pp. 284-289, 2013.

[10] Eletronuclear, "Panorama da energia nuclear no mundo",Available in:
<http://www.eletronuclear.gov.br/LinkClick.aspx?fileticket=SG_9CnL80wM%3d&tabid=40>. Access in: January 25, 2017.

[11] G. Nyalunga, V. Naicker, M. Toit,"Developing skills for neutronic modelling of nuclear power reactors in South Africa", Journal of energy in Souther Africa, vol. 4, pp. 27, 2016.

[12] A.M. Xavier, A.G. Lima, C.R.M. Vigna, F.M. Verbi, G.G. Bortoleto, K. Goraieb, C.H. Collins, M.I.M.S. Bueno, "Landmarks in the history of radioactivity and current tendencies", Química Nova, vol. 1, pp. 30, 2007.

[13] S.V. Yudintsev, S.V. Stefanovsky, B.S. Nikonov, "A pyrochlore-based matrix for isolation of the REE-actinide fraction of wastes from spent nuclear fuel reprocessing", Doklady Earth Sci., vol. 454, pp. 54-58, 2014.

[14] J.P. Ackerman, L.S.H. Chow, S.M. McDeavitt, C. Pereira, R.H. Woodman, "Isolating wastes in the electrometallurgical treatment of spent nuclear fuel", JOM, vol. 49, pp. 26-28, 1997.

[15] T.B. Kirchner, J.L. Webb, S.B. Webb, R. Arimoto, D.A. Schoep, B.D. Stewart, "Variability in background levels of surface soil radionuclides in the vicinity of the US DOE waste isolation pilot plant", J. Environmental Radioactivity, vol. 60, pp. 275-291, 2002.

[16] S. Ullah, Z. Hussain, S. Mahboob, K. Al-ghanin, "Heavy Metals in Garragotyla, Cyprinuscarpio and Cyprinionwatsoni from the River Panjkora, District, Lower Dir, Khyber Pakhtunkhwa, Pakistan", Brazilian Archives of Biology and Technology, vol. 59, 2016.

[17] S.M.S.G. Nascimento, A.P. Souza, V.L.A. Lima, C.W.A. Nascimento, J.J.V.R. Nascimento, "Phytoextractor Potential of Cultivated Species in Industrial Area Contaminated by Lead", Revista. Brasileira de Ciência do Solo, vol. 40, 2016.

[18] F.R. Moreira, J.C. Moreira, "Os efeitos do chumbo sobre o organismo humano e seu significado para a saúde", Revista Panamericana de Salud Publica, vol. 15, pp. 119, 2004.

[19] Z. Said, A.A. Alshehhi, A. Mehmood, "Predictions of UAE's renewable energy mix in 2030", Renewable Energy, vol. 118, pp. 779-789, 2018.

[20] C.C. Azubuike, C.B. Chikere, G.C. Okpokwasili, "Bioremediation techniques-classification based on site of application: principles, advantages, limitations and prospects", World J. Microbiol. Biotechnol., vol. 32, 2016.

[21] N. Velmurugan, G. Hwang, M. Sathishkumar, T.K. Choi, K.J. Lee, B.T. Oh, Y.S. Lee, "Isolation, identification, Pb(II) biosorption isotherms and kinetics of a lead adsorbing Penicillium sp. MRF-1 from South Korean mine soil", J. Environmental Sci., vol. 22, pp. 1049-1056, 2010.

[22] X. Luo, X.C. Zeng, Z. He, X. Lu, J. Yuan, J. Shi, M. Liu, Y. Pan, Y.X. Wang, "Isolation and characterization of a radiation-resistant bacterium from Taklamakan Desert showing potent ability to accumulate Lead (II) and considerable potential for bioremediation of radioactive wastes", Ecotoxicology, vol. 23, pp. 1915-1921, 2014.

[23] Y.J. Park, Y.C. Lee, W.S. Shin, SJ Choi, "Adsorptive removal of cobalt, strontium and cesium using AMP-PAN in laundry wastewater from nuclear power plant", Abstracts of Papers of the American Chemical Society, vol. 237, pp. 193, 2009.

[24] R. Zarrougui, R. Mdimagh, N. Raouafi, "Highly efficient extraction and selective separation of uranium (VI) from transition metals using new class of undiluted ionic liquids based on H-phosphonate anions", J. Hazardous Mat., vol. 342, pp. 464-476, 2018.

[25] Ministério do Meio Ambiente - Conselho Nacional do Meio Ambiente, "Resolução n° 430, de 13 de maio de 2011",Available in: <http://www.mma.gov.br/port/conama/legiabre.cfm?codlegi=646>. Access in: September 8, 2017.

[26] K.L. Plathe, F.V.D. Kammer, M. Hassello, J.N. Moore, M. Murayama, T. Hofmann, M.F. Hochella Jr, "The role of nanominerals and mineral nanoparticles in the transport of toxic trace metals: Field-flow fractionation and analytical TEM analyses after nanoparticle isolation and density separation", Geochimica et Cosmochimica Acta, vol. 102, pp. 213-225, 2013.

[27] Y. PAN, M.E. FLEET, N.D. MACRAE, "Late alteration in titanite (CaTiSiOS): Redistribution and remobilization of rare Earth elements and implications for U/Pb and Th/Pb geochronology and nuclear waste disposal", Geochimica et Cosmochimica Acta, vol. 57, pp. 355-367, 1993.

[28] J. Huang, K. Nara, C. Lian, K. Zong, K. Peng, S. Xue, Z. Shen, "Ectomycorrhizal fungal communities associated with Masson pine (Pinus massoniana Lamb.) in Pb-Zn mine sites of central south China", Mycorrhiza, vol. 22, pp 589-602, 2012.

[29] E.S. Eitrheim, "Characterization of wastes pertaining to naturally occurring radioactive materials (NORM) and the nuclear fuel cycle", Msc. Thesis, University of Iowa, 2017.

[30] E.R. Pereira Filho, "Planejamento fatorial em química: Maximizando a obtenção de resultados", 1ª. ed., UFSCAR: São Carlos, 2015.

[31] R.F. Gunst, R.L. Mason, "Fractional factorial design", Wiley Online Library, vol. 1, pp. 234-244, 2009.

[32] N. AlMasoud, E. Correa, D.K. Trivedi, R. Goodacre, "Fractional Factorial Design of MALDI-TOF-MS Sample Preparations for the Optimized Detection of Phospholipids and Acylglycerols", Anal. Chem., vol. 88, pp 6301-6308, 2016.

[33] J.A. Barminko, N.I. Nativ, R. Schloss, M.L. Yarmush, "Fractional factorial design to investigate stromal cell regulation of macrophage plasticity", Wiley Online Library, vol. 111, pp. 2239-2251, 2014.

[34] J. Yu, Q. Wang, Z. Zhang, X. Li, "Multi-objective optimizations of multidirectional forming mold based on fractional factorial design", The International J. Advanced Manufacturing Technol., vol. 88, pp 1151-1160, 2017.

[35] M.W.M. Cunico, M.M. Cunico, O.G. Miguel, S.F. Zawadzki, P. Peralta-Zamora, N. Volpato, "Planejamento fatorial: uma ferramenta estatística valiosa para a definição de parâmetros experimentais empregados na pesquisa científica", Visão Acadêmica, vol. 1, pp. 9, 2008.

[36] S. Olivier, V.L. Silva, M. Motta, J.E. Silva, "Emprego de planejamento fatorial no desenvolvimento de uma metodologia para extração de zinco de resíduos galvânicos", Química nova, vol. 7, pp. 30, 2007.

[37] A. Rai, B. Mohanty, R. Bhargava, "Supercritical extraction of sunflower oil: A central composite design for extraction variables", Food Chemistry, vol. 192, pp. 647-659, 2016.

[38] P. Izadiyan, B. Hemmateenejad, "Multi-response optimization of factors affecting ultrasonic assisted extraction from Iranian basil using central composite design", Food Chemistry, vol. 190, pp. 864-870, 2016.

[39] J. Meijide, E. Rosales, M. Pazos, M.A. Sanromán, "p-Nitrophenol degradation by electro-Fenton process: Pathway, kinetic model and optimization using central composite design", Chemosphere, vol. 185, pp. 726-736, 2017.

[40] F. Nemati, R. Zare-Dorabei, M. Hosseini, M.R. Ganjali, "Fluorescence turn-on sensing of thiamine based on Arginine - functionalized graphene quantum dots (Arg-GQDs): Central composite design for process optimization", Sensors and Actuators B: Chemical, vol. 255, pp. 2078-2085, 2018.

[41] Minitab, versão 16.2.4.4, "Statiscal Software", Minitab Inc., 2013.

[42] E.T. Ozer, S. Guçer, "Central composite design for the optimisation of Cd and Pb determination in PVC materials by atomic absorption spectrometry after Kjeldahl digestion", Polymertesting, vol. 30, pp. 773, 2011.

[43] H. Sakurai, J. Noro, A. Kawase, M. Fujinami, K. Oguma, "Digestion of plastic materials for the determination of toxic metals with a microwave oven for house hold use", Anais. Sci., vol. 22, pp. 225, 2006.

[44] OriginPro, versão 9.1.0, "Data analysis and graphing software", Origin Lab Corporation, 1991-2013.

[45] I.M. Savic, S.T. Stojiljkovic, D.G. Gajic, "Modeling and optimization of energy-efficient procedures for removing lead(II) and zinc(II) ions from aqueous solutions using the central composite design", Energy vol. 77, pp. 66, 2014.

[46] R. Zare-Dorabei, S.M. Ferdowsi, A. Barzin, A. Tadjarodi, "Highly efficient simultaneous ultrasonic-assisted adsorption of Pb(II),Cd(II), Ni(II) and Cu (II) ions from aqueous solutions by graphene oxidemodified with 2,20-dipyridylamine: Central composite designoptimization", Ultrasonics Sono Chemistry, vol. 32, pp. 265, 2016.